JOURNAL OF MATERIALS SCIENCE **36** (2001) 1601–1607

Abrasive wear behaviour of zinc-aluminium alloy - 10% Al_2O_3 composite through factorial design of experiment

O. P. MODI, R. P. YADAV, D. P. MONDAL, R. DASGUPTA, S. DAS, A. H. YEGNESWARAN
Regional Research Laboratory (CSIR), Hoshangabad Road, Near Habibganj Naka, Bhopal - 462 026, India
E-mail: opmodi@rrlbpl.org

Two body abrasive wear behaviour of a zinc-aluminium alloy - 10% Al_2O_3 composite was studied at different loads (1–7 N) and abrasive sizes (20–275 μm) as a function of sliding distance and compared with the matrix alloy. The wear rate of the composite and the matrix alloy has been expressed in terms of the applied load, abrasive size and sliding distance using linear factorial design approach. The study suggests that the wear rate of the alloy and composite follow the following relations:

$$Y_{\text{alloy}} = 0.1334 - 0.0336x_1 + 0.0907x_2 + 0.0219x_3 - 0.0296x_1x_2 + 0.0274x_2x_3 - 0.0106x_3x_1 - 0.0201x_1x_2x_3$$

$$Y_{\text{comp}} = 0.0726 - 0.028x_1 + 0.062x_2 + 0.03x_3 - 0.024x_1x_2 + 0.028x_2x_3 - 0.016x_3x_1 - 0.014x_1x_2x_3$$

where, x_1, x_2 and x_3 are the coded values of sliding distance, applied load and abrasive size respectively. It has been demonstrated through the above equations that the wear rate increases with applied load and abrasive size but decreases with sliding distance. The interaction effect of the variables exhibited a mixed behaviour towards the wear of the material. It was also noted that the effect of load is less prominent for the composite than the matrix alloy while the trend reversed as far as the influence of the abrasive size is concerned.

1. Introduction

Zinc-aluminium alloys have emerged as excellent substitutes to many ferrous and non ferrous alloys for different engineering applications because of their excellent castability, light weight and superior mechanical and wear properties [1–6]. However, one of the major limitations of these alloys have been deterioration in mechanical and tribological properties at temperatures above 100°C [7, 8]. The alloys have also been found to suffer from abrasion caused by entrapped particles in related applications. The problem of deterioration of the above mentioned properties has been suggested to be reduced through microstructural modifications of the alloys by adding high melting elements like Ni, Si etc. [9, 10]. Incorporation of hard second phase (SPPs) particles in the alloy matrix to form composites has also been reported to be more beneficial in this context [7, 11, 12]. The particles not only impart excellent abrasion resistance but also improve elevated temperature properties of the zinc-based alloys [13–19]. The abrasive wear behaviour of alloys containing hard SSPs greatly depends on factors like (i) nature, shape, size, hardness and rake angle of the abrading particles; (ii) nature, shape, size, hardness, volume fraction and distribution of the second phase particles (SSPs) in the matrix; (iii) properties of the matrix; (iv) nature of dispersoid/matrix interfacial bonding; and (v) experimental conditions such as abrasive size, applied load, sliding speed and sliding distance [13, 15].

It has been reported that the extent of plastic deformation in the subsurface regions depends on the abrasive size as well as on applied load [14, 15, 20–22]. Further, high load and coarse abrasive size (coarser than dispersoid phase) may result in lower wear resistance of zinc-aluminium alloy - silicon carbide composite as compared to the matrix alloy [22].

Abrasive wear rate is expressed in terms of hardness and applied load by the following relation [23]:

$$W = \frac{K\varepsilon_{\text{deff}}P}{\varepsilon_{\text{coef}}H} \quad (1)$$

where K - wear coefficient defined as the probability of formation of wear particles, P - applied load, H-material hardness, $\varepsilon_{\text{deff}}$ - strains at which asperities undergoing plastic deformation and $\varepsilon_{\text{coef}}$ - strains associated with crack growth within asperities. The equation suggests that not only the hardness, but also the plastic deformation and fracture toughness ($\varepsilon_{\text{coef}}$) of a material influence the wear behaviour. The material removal mechanism during abrasive wear has also been explained on the basis of fracture toughness, plasticity and friction [24]. It is reported by several investigators that wear rate of a material also varies with load, sliding distance and abrasive size [20–22]. However, attempts made to correlate wear rate with the combined effect of these factors are limited [25]. Further, no information exists in this regard as far as zinc-based alloys/composites are concerned. The abrasive wear rate of aluminium composite and matrix alloy in terms of load and abrasive size following a factorial design approach has been predicted by Mondal *et al*. [25]. However, this study did not consider the effect of sliding distance on wear behaviour whereas the wear rate depends on sliding distance considerably. Available information suggests that it is possible to assess quantitatively the influence of each of the above variables (load, abrasive size and sliding distance) separately or in combination on the wear rate by deriving some emperical equations involving statistical analysis of the recorded data through factorial design of experiments.

In view of the above, the present study aims to develop a regression equation for (i) assessing the high stress abrasive wear rate of a zinc-aluminium alloy-Al_2O_3 particle composite vis-a-vis the matrix alloy as a function of the variables like sliding distance, load and abrasive size, (ii) comparing the effect of each variable and their interaction on the wear rate of each of the material, and (iii) assessing the extent of deviation of theoretically calculated values of wear rate over the experimentally observed ones.

2. Experimental

2.1. Material

The zinc-based alloy (Zn - 37.2% Al – 2.5% Cu – 0.2% Mg) was dispersed with 10 wt.% Al_2O_3 particles (size 75–150 μm) to synthesize the composite by a liquid metallurgy route using the vortex technique. The composite melt was cast in the form of 6 mm thick, 120 mm diameter disc using cast iron moulds. The matrix alloy was also processed under identical conditions for a comparative study. Metallographically polished specimens were etched with diluted aqua regia and examined under scanning electron microscope.

2.2. Abrasive wear tests

High-stress abrasive wear tests were performed on metallographically polished rectangular specimens (size: $40 \times 35 \times 4$ mm^3) using a suga (Japan) make abrasion tester (Model: NUS 1; Japan). Fig. 1 shows a schematic view of the high stress (two body) abrasion test apparatus. The SiC particles, embedded on an emery paper and fixed on a 50 mm diameter and 12 mm thick aluminium wheel with the help of a double sided tape was used as the abrasive medium. The samples were loaded against the abrasive medium with the help of a cantilever mechanism. The specimens experienced to-and-fro motion against the abrasive particles while the abrasive wheel also changed its position by the time the specimens completed one cycle (corresponding to a sliding distance of 0.065 m). This enabled the samples to encounter fresh abrasive particles (in each cycle) prior to traversing 400 cycles (corresponding to a sliding distance of 25 m). Beyond this distance, degraded abrasive came in contact with the specimen surface in succession. Abrasive wear tests were conducted for 400, 800, 1200, 1600 and 2000 cycles, corresponding sliding distances being 25, 50, 75, 100 and 125 m respectively. A range of applied loads (1–7 N) and abrasive sizes (23–275 μm) were employed while sliding velocity was fixed at 0.04 m/s for carrying out the tests. The specimens were ultrasonically cleaned with acetone prior to and after the wear tests. Weight loss of the specimens was measured using a Mettler micro balance for computing the wear rate.

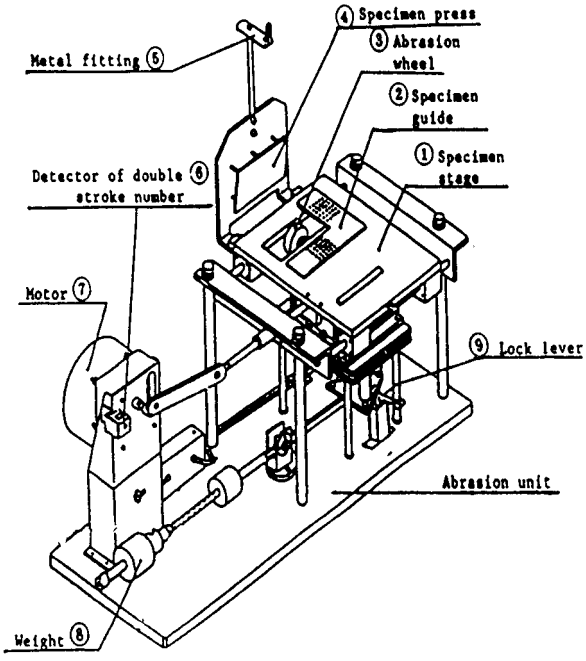

Figure 1 A schematic view of the high stress (two body) abrasion test apparatus.

2.3. Factorial design of experiments

A factorial design of experiment of the type P^n [25, 26] was used in the present study where 'n' corresponds to the number of factors and 'P' stands for the number of levels. In this design, $n = 3$ (i.e. sliding distance, applied load and abrasive size) and $P = 2$ (i.e. upper and lower levels of each variable). Thus the minimum number of trial experiments to be conducted for each material is $2^3 = 8$. If wear rate is represented by Y, the linear regression equation for these experiments could be written as

$$Y = a_0 + a_1x_1 + a_2x_2 + a_3x_3 + a_4x_1x_2 + a_5x_2x_3 + a_6x_1x_3 + a_7x_1x_2x_3 \quad (2)$$

where a_0 is the response variable (wear rate) at the base level (i.e. at the sliding distance of 75 m, load of 4 N and abrasive size of 149 μm); a_1, a_2, a_3 are coefficients associated with each variable x_1 (sliding distance), x_2 (applied load) and x_3 (abrasive size); and a_4, a_5, a_6, a_7 are interaction coefficients between x_1 and x_2, x_2 and x_3, x_1 and x_3, and x_1, x_2 and x_3 respectively within the selected levels of each of the variables.

The positive value of 'Y' from Equation 2 denotes weight loss while its negative value indicates weight gain. Further, the positive value of any of the coefficients suggests that the wear rate of material increases with their associated variables while their magnitude indicates the weightage of each of these factors or their interaction towards the wear rate of the material. x_1, x_2 and x_3 in the equation are the coded values of sliding distance, applied load and abrasive size. The coded value for a particular variable is defined as follows:

$$\text{Coded Value} = \frac{\text{base value} - \text{selected value}}{|\text{base value} - \text{value corresponding to lower or upper level}|}$$

The procedure for calculating each of the above mentioned coefficients in Equation 2 has been reported elsewhere [25, 26].

3. Results

3.1. Microstructure

Fig. 2 shows the microstructural features of the composite. Reasonably uniform distribution of dispersoid particles (Al_2O_3) may be seen in Fig. 2a while defect free dispersoid/matrix interfacial bonding may be seen in the magnified micrograph (Fig. 2b).

3.2. Abrasive wear behaviour

Fig. 3 represents the wear rate of the samples as a function of travel distance at different applied loads and for various abrasive sizes. It is noted that the wear rate of composite is less than that of the alloy irrespective of applied load and abrasive size. Furthermore, it may be noted that wear rate of these materials decreases with sliding distance and increases with applied load and abrasive size. However, the combined effect of these parameters on the wear rate can not be understood from such type of plots. Hence, these data are subjected to factorial design with an aim to establish an emperical relation for wear rate as a function of applied load, sliding distance and abrasive size.

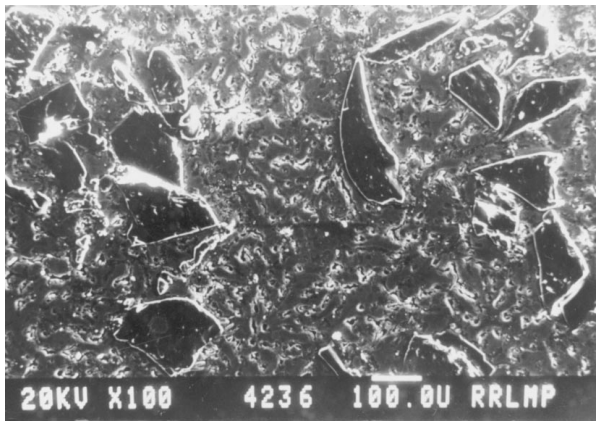

(a)

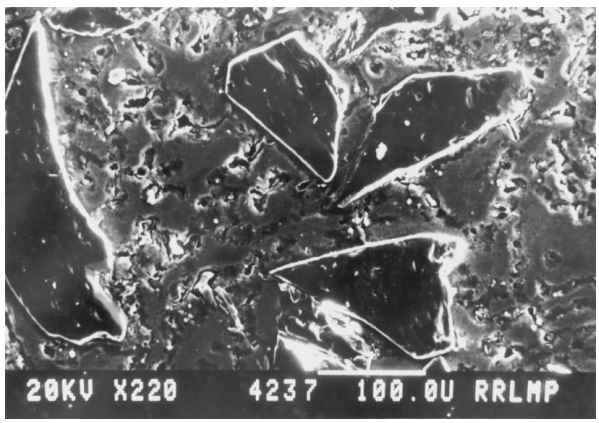

(b)

Figure 2 Optical micrographs of the ZA37-10 Al_2O_3 composite showing (a) distribution of dispersoid phase in the alloy matrix and (b) dispersoid/matrix interfacial bonding.

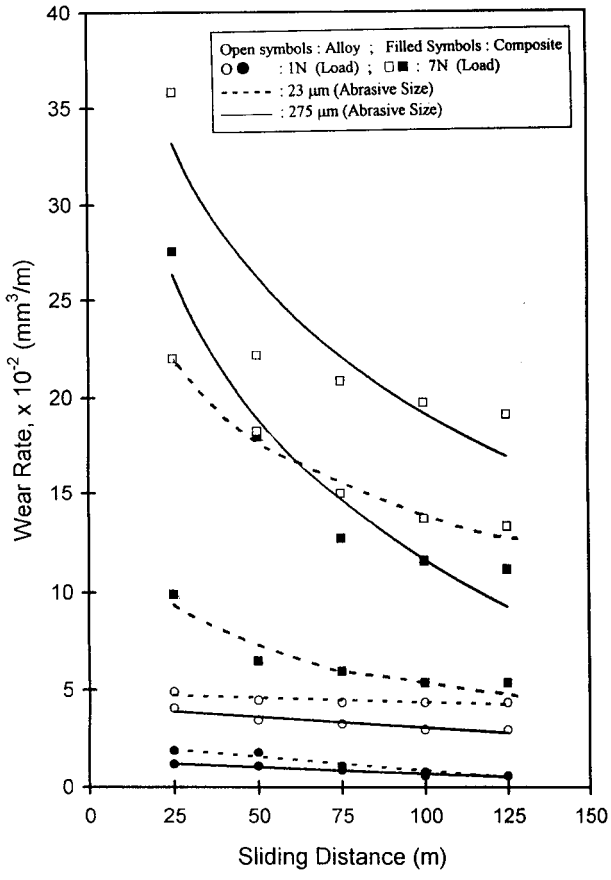

Figure 3 Wear rate as a function of sliding distance at different applied loads and abrasive sizes.

TABLE I Levels of each factor and their coded values

Sl. No.	Factor Levels Coded Values	Variables: Sliding Distance (m) x_1	Applied Load (N) x_2	Abrasive Size (μm) x_3
1	Upper level (Coded value)	125 (+1)	7 (+1)	275 (+1)
2	Base level (Coded value)	75 (0)	4 (0)	149 (0)
3	Lower level (Coded value)	25 (−1)	1 (−1)	23 (−1)

TABLE II The value of individual variable with their coded value and wear response in each trial

Trial No.	Sliding Distance (m) x_1	Appled Load (N) x_2	Abrasive Size (μm) x_3	Wear Rate (m^3/m) Y_{alloy}	Y_{comp}
1	+1 (125)	+1 (7)	+1 (275)	0.192	0.112
2	+1 (125)	+1 (7)	−1 (23)	0.133	0.054
3	+1 (125)	−1 (1)	−1 (23)	0.044	0.006
4	−1 (125)	−1 (1)	−1 (23)	0.049	0.011
5	−1 (25)	+1 (7)	+1 (275)	0.358	0.275
6	−1 (25)	−1 (1)	+1 (275)	0.041	0.018
7	+1 (125)	−1 (1)	+1 (275)	0.03	0.006
8	−1 (25)	+1 (1)	−1 (23)	0.22	0.0099

Values in the parenthesis are the actual values of the experimental parameters.

TABLE III Matrix design for calculating regression coefficients

Sl. No.	x_1	x_2	x_3	x_1x_2	x_2x_3	x_3x_1	$x_1x_2x_3$	Y_{alloy}	$Y_{composite}$
1	+1	+1	+1	+1	+1	+1	+1	0.192	0.112
2	+1	+1	−1	+1	−1	−1	−1	0.133	0.054
3	+1	−1	−1	−1	+1	−1	+1	0.044	0.006
4	−1	−1	−1	+1	+1	+1	−1	0.049	0.011
5	−1	+1	+1	−1	+1	−1	−1	0.358	0.275
6	−1	−1	+1	+1	−1	−1	+1	0.041	0.018
7	+1	−1	+1	−1	−1	+1	−1	0.03	0.006
8	−1	+1	−1	−1	−1	+1	+1	0.22	0.099

Upper, lower and base levels of the variables along with their coded values are shown in Table I. The factorial design of experiments and the values of response variables corresponding to each set of trials are represented in Table II. The matrix design for calculating each of the coefficients in Equation 2 for the specimens is mentioned in Table III.

After calculating each of the coefficients of Equation 2, the final linear regression equation for the wear rate of the alloy and composite can be expressed as follows:

$$Y_{alloy} = 0.1334 - 0.0336x_1 + 0.0907x_2 + 0.0219x_3 - 0.0296x_1x_2 + 0.0274x_2x_3 - 0.0106x_3x_1 - 0.0201x_1x_2x_3 \quad (3)$$

$$Y_{comp} = 0.0726 - 0.028x_1 + 0.062x_2 + 0.03x_3 - 0.024x_1x_2 + 0.028x_2x_3 - 0.016x_3x_1 - 0.014x_1x_2x_3 \quad (4)$$

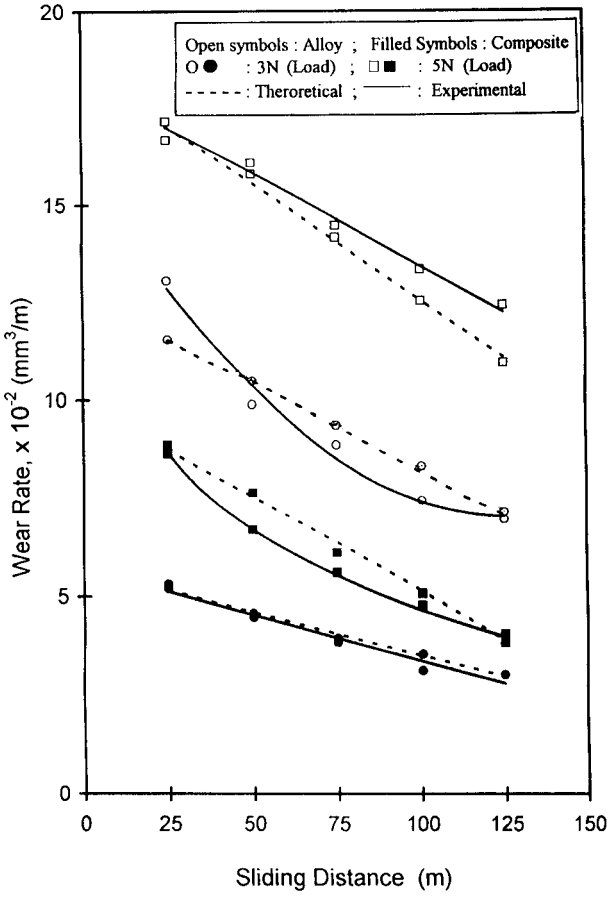

Figure 4 Wear rate as a function of sliding distance showing the comparison between the theoretical and experimental values.

Substituting the coded values of the variables for any experimental condition in Equations 3 and 4, the wear rate of the matrix alloy and composite can be calculated. Table IV shows the calculated values along with the experimental values in different experimental conditions. By comparing theoretical and experimental values from Table IV, it can clearly be observed that theoretical values differ from the experimental values within ±10%. Once again the calculated values of wear rate along with the experimental values at different random experimental conditions were plotted as a function of sliding distance in Fig. 4. It is also evident from this figure that the calculated values are in close proximity with the experimental ones. These facts suggest reasonably good reliability of the equations to predict the wear rate of the samples within the selected experimental domains.

4. Discussion

In two body abrasion, the abrasive particles are rigidly fixed on an emery paper/cloth against which the specimen surface moves. As a result, the abrasive particles cannot move freely or change their position against the specimen surface during the tests. This results in most efficient load transfer from the abrasive medium to the specimen surface. As a consequence, high stress condition is created in this mode of wear and the individual abrasive particle penetrates into the specimen surface to the same depth irrespective of the nature of the microconstituents present in the material [27]. However,

TABLE IV Results of random experiments and its corresponding theoretical values

Exp. No.	Variables: Sliding distance (m) x_1	Load (N) x_2	Abrasive. Size (μm) x_3	Wear Rate (m^3/m): Y_{alloy}	Y_{comp}
1	100 (0.5)	3 (−0.33)	65 (−0.67)	0.0894 (0.0838)	0.0319 (0.044)
2	100 (0.5)	3 (−0.33)	40 (−0.865)	0.0822 (0.0822)	0.0288 (0.035)
3	50 (−0.5)	3 (−0.33)	65 (−0.67)	0.098 (0.105)	0.0452 (0.057)
4	50 (−0.5)	3 (−0.33)	40 (−0.865)	0.974 (0.102)	0.039 (0.045)
5	100 (0.5)	5 (0.33)	65 (−0.67)	0.139 (0.126)	0.055 (0.048)
6	100 (0.5)	5 (0.33)	40 (−0.865)	0.124 (0.122)	0.049 (0.042)
7	50 (−0.5)	5 (0.33)	65 (−0.67)	0.161 (0.158)	0.078 (0.077)
8	50 (−0.5)	5 (0.33)	40 (−0.865)	0.136 (0.150)	0.063 (0.067)

Values in the parenthesis are coded values of the experimental parameters and calculated wear rates from linear regression equations.

the depth of penetration is a function of several factors [16–25] like applied stress, rake angle of the abrasive particles and relative hardness and size of the abrasive with respect to that of the dispersoid particles as well as on overall hardness of the specimen surface. The depth of penetration increases with increasing abrasive size, rake angle and effective stress on the abrasive. These result in increasing cutting efficiency of the abrasive particles. On the contrary, increasing hardness of the test materials produces a reverse effect in view of the resistance offered by the surface against the penetrating action of the abrasive particles [21]. In the case of the presence of hard second phase particles in the alloy matrix (i.e. composite), the reinforced hard particles reduce the extent of penetration of the abrasive particles on the specimen surface thereby protecting the softer matrix surrounding the hard second phase [28]. Even if the abrasive penetrates into the softer matrix, the hard second phase particles offer resistance against the movement of the penetrated abrasive on the specimen surface. Thus, the composite attains lower wear rate than the matrix alloy [13–15]. However, this trend is maintained as long as the dispersoid phase is retained by the alloy matrix. Such a situation is favoured when the depth and width of groove made by the abrasive particles are smaller than the size of the dispersoid particles. Thus, the effect of dispersoid towards reduction in wear rate becomes more effective when the abrasive size are smaller than the size of the dispersoid [13, 14, 20, 21]. On the contrary, when the tests are conducted against abrasive particles coarser than the dispersoid phase there is a greater possibility of scooping out or fracture/fragmentation of the dispersoid phase by the (coarser) abrasive particles causing the composite to suffer from higher wear rate than that of the matrix alloy [13, 14, 20, 21]. However, in the present experimental domain, the composite exhibited higher wear resistance than the matrix alloy despite of using coarser abrasive size than the dispersoid phase even at higher applied load. This could be attributed to stronger interfacial bonding between the dispersoid/matrix interface as well as greater capacity to hold the dispersoid phase by the matrix (Fig. 2b). Further, the hardness of alumina dispersoid is relatively lower than that of the SiC abrasive causing formation of finer alumina fragments which are easily picked up in the matrix portion of the wear surface of the composite. This would facilitate the formation of thicker, stable and harder composite layer finally leading to less wear of the composite than matrix alloy even at higher load and coarser abrasive size.

Another factor affecting the wear behaviour is travel distance. In the present study, the degraded abrasive came in contact with the specimen surface in succession of a travel distance of 25 m. Under these circumstances, the cutting efficiency of the abrasive deteriorated gradually with the sliding distance through increase extent of capping, clogging, attrition and shelling as discussed elsewhere [29, 30]. Accordingly, the wear rate decreases with sliding distance. The extent of reduction in the wear rate with distance is less in the case of the composite over that of the matrix alloy (Figs 3 and 4) in view of more severe degradation of the abrasive medium with sliding distance when the abrasives move over the alloy due to higher degree of capping and clogging. As relatively finer microcutting chips are produced and the matrix is plastically constrained, chances of capping and clogging of the abrasive is relatively less in the case of composite.

A comparison of the coefficient a_0 for the composite and matrix alloy demonstrates that at the base level (i.e. load: 4 N, abrasive size: 149 μm and sliding distance: 75 m), the wear rate of the composite (0.0726×10^{-11} m^3/m) is lower than that of the alloy (0.1334×10^{-11} m^3/m). This behaviour is in line with the trend observed under various experimental conditions and has been explained earlier.

The coefficient (a_1) associated with sliding distance (x_1) is noted to be negative for both kinds of the specimens. This suggests that the wear rate decreased with increasing traversal distance and could be explained on the basis of the experiments conducted in this study and degradation of abrasive media with sliding distance as stated earlier. Here the abrasive medium completes one rotation after every 400 cycles. As a result, after 400 cycles, used abrasive comes in contact with the specimen surface. Accordingly, its cutting efficiency is reduced with increasing sliding distance beyond the first 400 cycles due to aforesaid reasons.

The predicted wear behaviour of the samples has been found to lie close to that of the experimentally observed ones. For example, the coefficients a_2 and a_3 associated with the applied load (x_2) and abrasive size (x_3) were found to be positive which indicate that wear rate increases with load and abrasive size (Figs 3 and 4) and decreases with sliding distance. The calculated values of wear rate for alloy and composite at 3 N and 5 N

load with the experimental values under these loading conditions at 65 μm abrasive size are plotted in Fig. 4. It demonstrates close proximity between the theoretical and experimental values.

It may be noted from Equations 3 and 4 that load has more adverse effect on the wear rate irrespective of the material. Further, it has been observed that the depth of penetration of the abrasive into the specimen surface increases with increase in abrasive size causing the cutting efficiency of the abrasive to increase. But, at the same time, number of abrasive particles at specific surface area reduces with increase in abrasive size. As a result the over all effect of abrasive size towards material removal is less significant as compared to that of applied load on the wear rate. As far as the effect of load is concerned, the depth of penetration is likely to increase with increase in applied load. This is in view of the fact that the abrasive particles are rigidly fixed on paper or cloth and the load is effectively transferred from abrasive to the specimen surface. However, the effect of load is noted to be more severe in the alloy while that of abrasive size may be more severe in the composite. Furthermore, the extent of clogging and capping decreases with increase in abrasive size which is expected to be more effective for the matrix alloy. It may also be noted that there is a greater chance of blunting and shelling of abrasives while abrading the composite thereby reducing the cutting efficiency of the abrasives due to the presence of hard second phase. The possibilities of these phenomena may be increasing with increase in applied load. Under higher applied load there is a greater possibility of fracture and fragmentation of the dispersoids which results in the removal of the dispersoid particles from the matrix resulting in higher wear rate. However, at the same time some of the broken dispersoid particles are picked up at the wear surface and again protect the surface from excessive wear. This phenomena is possible when the test is conducted against finer abrasive. If the abrasives are coarse enough to produce wear grooves wider than these fragmented dispersoids or the original dispersoid, then these particles are removed easily resulting in higher wear rate of the composite. If, the applied load is increased, the effective stress on the individual second phase particles increases and above a critical value these particles fracture/fragment. That is why the effect of abrasive size and the interaction effect of abrasive size and load is more severe for the composite than that observed in the alloy.

In comparison to the coefficients associated with single variable, the interaction coefficients of different variables towards the wear rate are also quite significant. Earlier we have already noticed that the coefficient associated with load and abrasive size is positive while that with distance is negative. This suggests sliding distance to be more effective than load and abrasive size in controlling the wear behaviour of the samples. The interaction coefficient between load and sliding distance is negative for the composite as well as the matrix alloy. It emerges that processes like the shelling, capping, clogging and work hardening become more effective at longer sliding distances with increasing combined effect of load and sliding distance and hence results in lower wear rate of the specimens.

The interaction coefficient between abrasive size and load is positive for both the varieties of samples. This clearly indicates that the combined action of load and abrasive size causes more damage to the specimen surface. This may be attributed to the fact that under high load and coarser abrasive size, cutting efficiency of the abrasive increases and causes the formation of wider and deeper wear grooves. However, this effect is relatively high in the case of composite. This could be attributed to greater chances of fracture/fragmentation and removal of hard dispersoid from the composite surface under the combined action of coarser abrasive and higher applied load.

The interaction coefficient between abrasive size and sliding distance is noted to be negative for both the alloy and composite. This signifies that the effect of abrasive size is less predominant than that of the sliding distance. Effects of the parameters on the wear behaviour of the samples can be explained as earlier. The possibility of clogging, capping, shelling and blunting of abrasive may not be varying significantly with the abrasive size. But, the possibility of these facts increases quite significantly with sliding distance. As a result, the wear rate decreases due to interaction of abrasive size and sliding distance. In the case of composite, this effect is more negative. This may be due to higher degree of shelling and blunting of abrasive due to the presence of hard dispersoid in it. Additionally, the clogged and capped material along with the coarser abrasive does not move for longer duration, rather they are released from the abrasive media after a very short duration.

Above equations thus describe the influence of each of the variables and their combined effects on the abrasive wear of the matrix alloy and composite in qualitative as well as in quantitative manner. The study suggests that one must take into consideration the interaction effects of all the variables to predict the wear response of the samples. In other words, this model enables to predict the wear behaviour of the samples as a function of load, abrasive size and sliding distance with fairly good level of confidence.

5. Conclusions

- Factorial design of experiment may be an important tool for describing two body abrasive wear behaviour of zinc-based alloy and composite in terms of different experimental variables like applied load, abrasive size and sliding distance. It is also helpful to understand the individual and combined effects of the parameters on the wear response of the samples.
- The established equations clearly demonstrate that composite exhibited higher wear resistance than the base alloy within the selected experimental domain.
- The effect of load was more severe for composite as compared to that of the matrix alloy, whereas the effect of abrasive on the wear rate of the composite was noted to be relatively less with respect to that

of the alloy. However, the wear rate of the samples increased with increasing load and abrasive size.

- The wear rate of the specimens decreased with increasing sliding distance. The rate of reduction in wear rate with sliding distance was more in the composite as compared to the matrix alloy.
- Interaction effects of the variables was quite considerable with respect to the effect of individual variables. Mixed effects of the interaction of the variables were also noticed. Interaction of abrasive size and sliding distance caused more wear rate of the matrix alloy but helped to reduce the wear rate of the composite. Similar behaviour was noticed for the combined effects of load, abrasive size and sliding distance.

Acknowledgment

Authors are thankful to Prof. T. C. Rao, Director, RRL, Bhopal for granting permission to publish this work.

References

1. T. S. CALAYAG, *Mining Engg.* **35** (1983) 727.
2. W. MIHAICHUK, *Machine Design* **53** (1981) 133.
3. D. APELIAN, M. PALIVAL and D. C. HERRSCHAFT, *J. Met.* **33** (1981) 12.
4. E. J. KUBEL JR., *Adv. Mater. Process.* **132** (1987) 51.
5. P. P. LEE, T. SAVASKAN and E. LAUFER, *Wear* **117** (1987) 79.
6. B. K. PRASAD, A. K. PATWARDHAN and A. H. YEGNESWARAN, *Z. Metallkd.* **87** (1996) 967.
7. M. A. DELLIS, J. P. KEUSTENRMANS and F. DELANNAY, *Mater. Sci. Eng.* **135A** (1991) 253.
8. W. MIHAICHUK, in Proc. 12th Int. Die Casting Congress and Exposition, Minneapolis, October/November 1983, paper No. GT 83-076 (Society of Die Casting Engrs. (SDCE), Inc. USA) p. 1.
9. B. K. PRASAD, Ph.D. Disertation, Met. Engg. Dept., University of Roorkee, India, 1994.
10. T. SAVASKAN and S. MURPHY, *Wear* **116** (1987) 211.
11. L. D. BAILEY, S. DIONNE and S. H. LO, in "Fundamental Relationship Between the Microstructure and Mechanical Properties of MMCs" edited by P. K. Liaw and M. N. Gungor (The Minerals, Metals and Materials Society, USA, 1990) p. 23.
12. A. A. DAS, A. J. CLEGG, B. ZANTONT and M. M. YAKOUB, in Proc. Cast Reinforced MMCs edited by S. G. Fishman and A. K. Dingra (ASM International, 1988) p. 139.
13. B. K. PRASAD, A. K. JHA, O. P. MODI, S. DAS and A. H. YEGNESWARAN, *Mater. Trans. JIM* **36** (1995) 1048.
14. B. K. PRASAD, S. V. PRASAD and A. A. DAS, *J. Mater. Sci.* **27** (1992) 4489.
15. *Idem. Mater. Sci. Engg.* **156A** (1992) 205.
16. O. P. MODI, B. K. PRASAD, A. H. YEGNESWARAN and M. L. VAIDYA, *ibid.* **151** (1992) 135.
17. S. DAS, S. V. PRASAD and T. R. RAMACHANDRAN, *Mater. Sci. Engg.* **138A** (1991) 123.
18. *Idem. Wear* **13** (1989) 173.
19. B. K. PRASAD, O. P. MODI and A. K. JHA, *Tribo. Int.* **27** (1994) 153.
20. M. A. MOORE, R. M. DOUTHWAITE, *Metall. Trans.* **7A** (1976)1833.
21. R. L. DEUIS, C. SUBRAMANIAN, J. M. YELLUP, *Wear* **201** (1996) 132.
22. B. K. PRASAD, S. DAS, A. K. JHA, O. P. MODI, R. DASGUPTA and A. H. YEGNESWARAN, *Composites* **28A** (1997) 301.
23. E. HORNBOGEN, *Wear* **33** (1975) 251.
24. A. G. ATKINS, in Fourth Tewsbury Symposium of Fracture, Melbourne University, February 1979, 17.1.
25. D. P. MONDAL, S. DAS, A. K. JHA and A. H. YEGNESWARAN, *Wear* **223** (1998) 131.
26. K. A. NATRAJAN, *Trans. Indian Inst. Met.* **42** (1989) 307.
27. T. KULIK, T. H. KOSEL and Y. XU, in Proc. Int. Conf. Wear Mater., Denver, April 1989, Vol. 1, edited by K. C. Ludema, p. 23.
28. S. V. PRASAD, P. K. ROHATGI and T. H. KOSEL, *Mater. Sci. Engg.* **80** (1986) 213.
29. A. P. MERCER and I. M. HUTCHINGS, *Wear* **132** (1989) 77.
30. A. MISHRA and I. FINNIE, *ibid.* **65** (1980) 369.

Received 5 July
and accepted 24 October 2000